Supporting Information

Hydrogel-based bioinks for cell electrowriting of well-organized living structures with micrometer-scale resolution

Miguel Castilho[a,b]†, Riccardo Levato[a,c]†, Paulina Nunez Bernal[a], Mylène de Ruijter[a], Christina Y. Sheng[a], Joost van Duijn[a], Susanna Piluso[a,d], Keita Ito[a,b], Jos Malda[a,c]*

* To whom correspondence should be addressed. E-mail: M.DiasCastilho@umcutrecht.nl

Supplementary Figures and Figure Captions

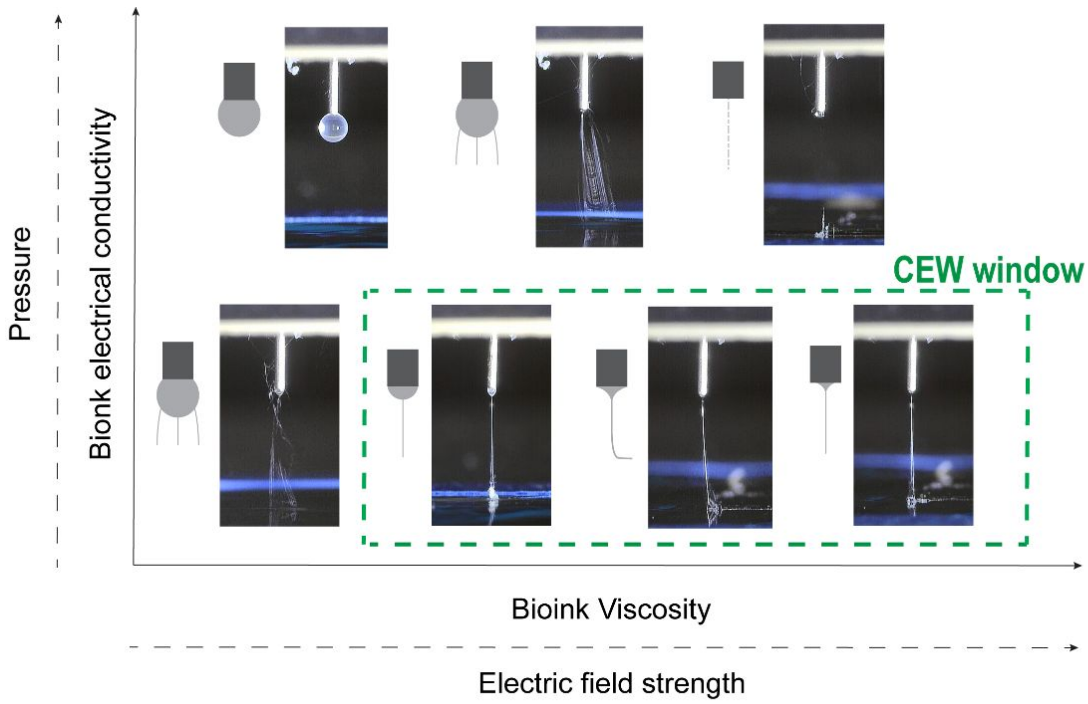

Figure S1: Cell electrowriting (CEW) fabrication window. Effect of key hydrogel materials properties and CEW processing parameters on the electrified jet formation. Quantitative investigation of bioink electrical conductivity and viscosity, as well as dispensing pressure, high voltage and collector velocity on CEW jet formation and fibre morphology and diameter can be found in Figures 2 and 3.

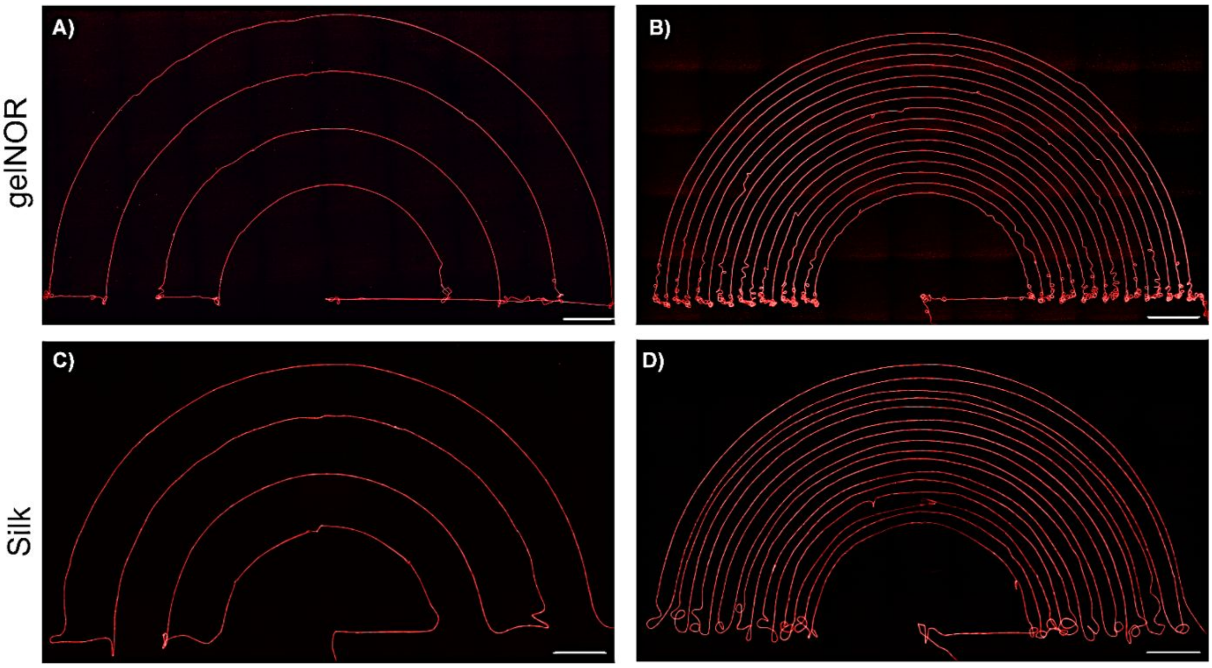

Figure S2: Representative microscopy images of curved CEW fibers of gelNOR (top) and silk (bottom). Curved fibers could be produced with an interfiber spacing of A-C) 1000 µm and B-D) 200 µm. Scale bar = 1000 µm

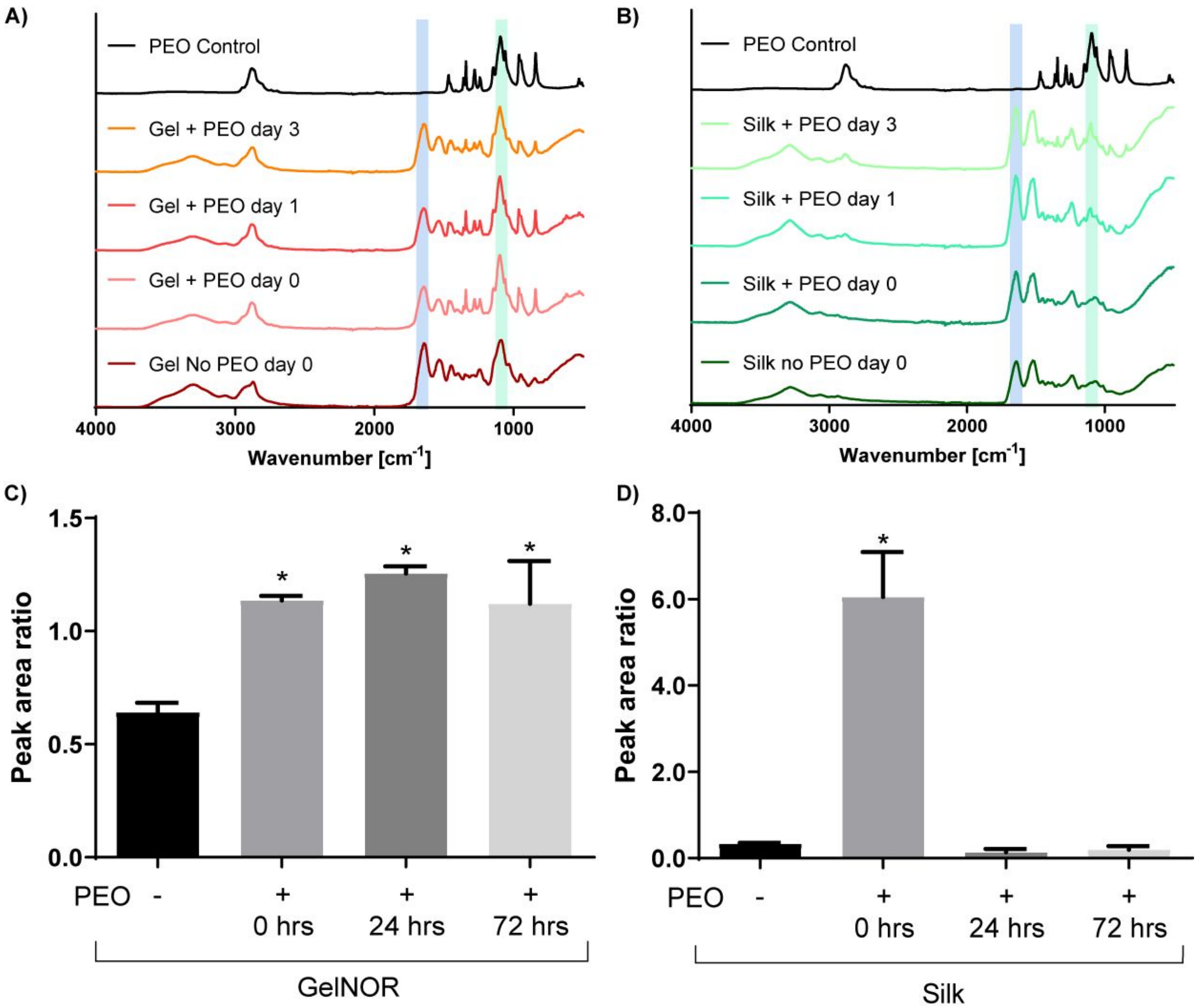

Figure S3: FTIR analysis of hydrogels formed from the (A) gelNOR and (B) Silk-based CEW bioinks before and after incubation in PBS for 0, 24 and 72 hours. The amide I band and the major ether bond stretching band are highlighted in blue and green, respectively. The ratio between the area under the asymmetric C-O-C stretching peak and the amide I band shows (C) presence of PEO within the gelNOR mixture, and (D) release of PEO after 1-day of incubation in PBS for the silk-based bioinks.

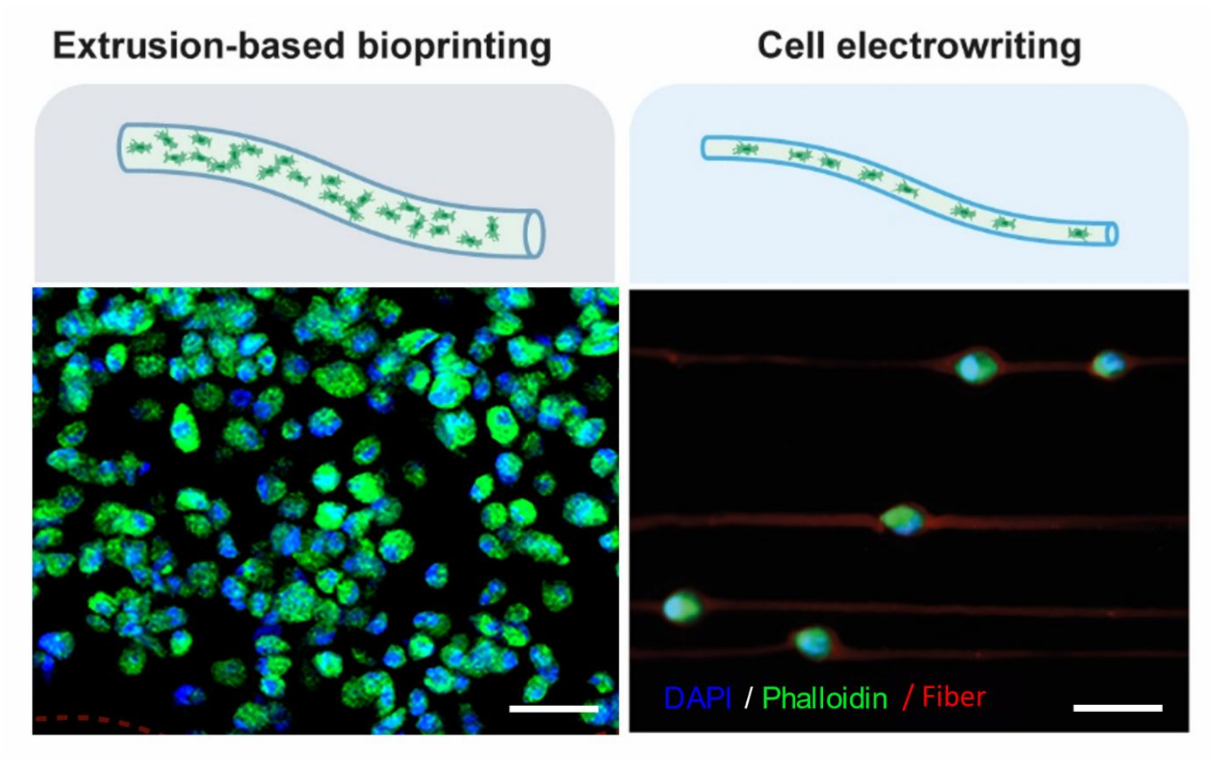

Figure S4: Representative fluorescence images of cells on gelNOR based cell-laden scaffolds obtained by conventional extrusion bioprinting (left) and CEW (right).

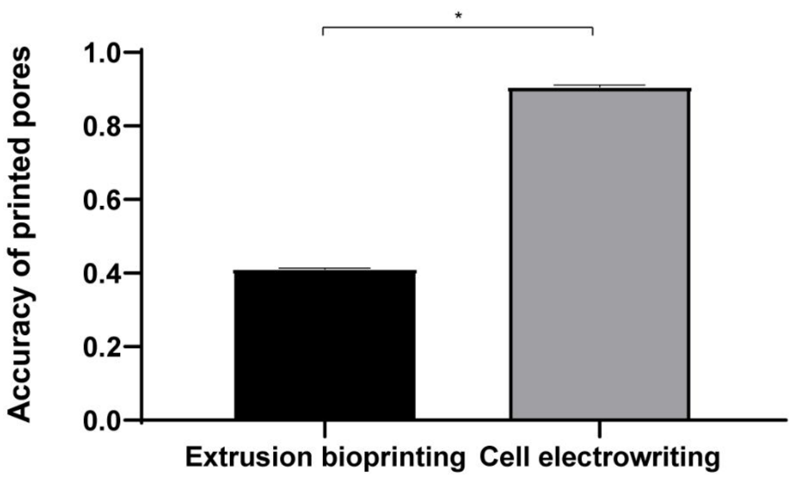

Figure S5: Comparison of printing accuracy of gelNOR scaffolds produced by extrusion bioprinting and cell electrowriting. Accuracy was determined using a relative value, $A_{cc\ pore}$, obtained by the ratio between the design and fabricated pore area. In the case of no deviation between printed and designed pore areas, $Acc_{pore} = 1$.

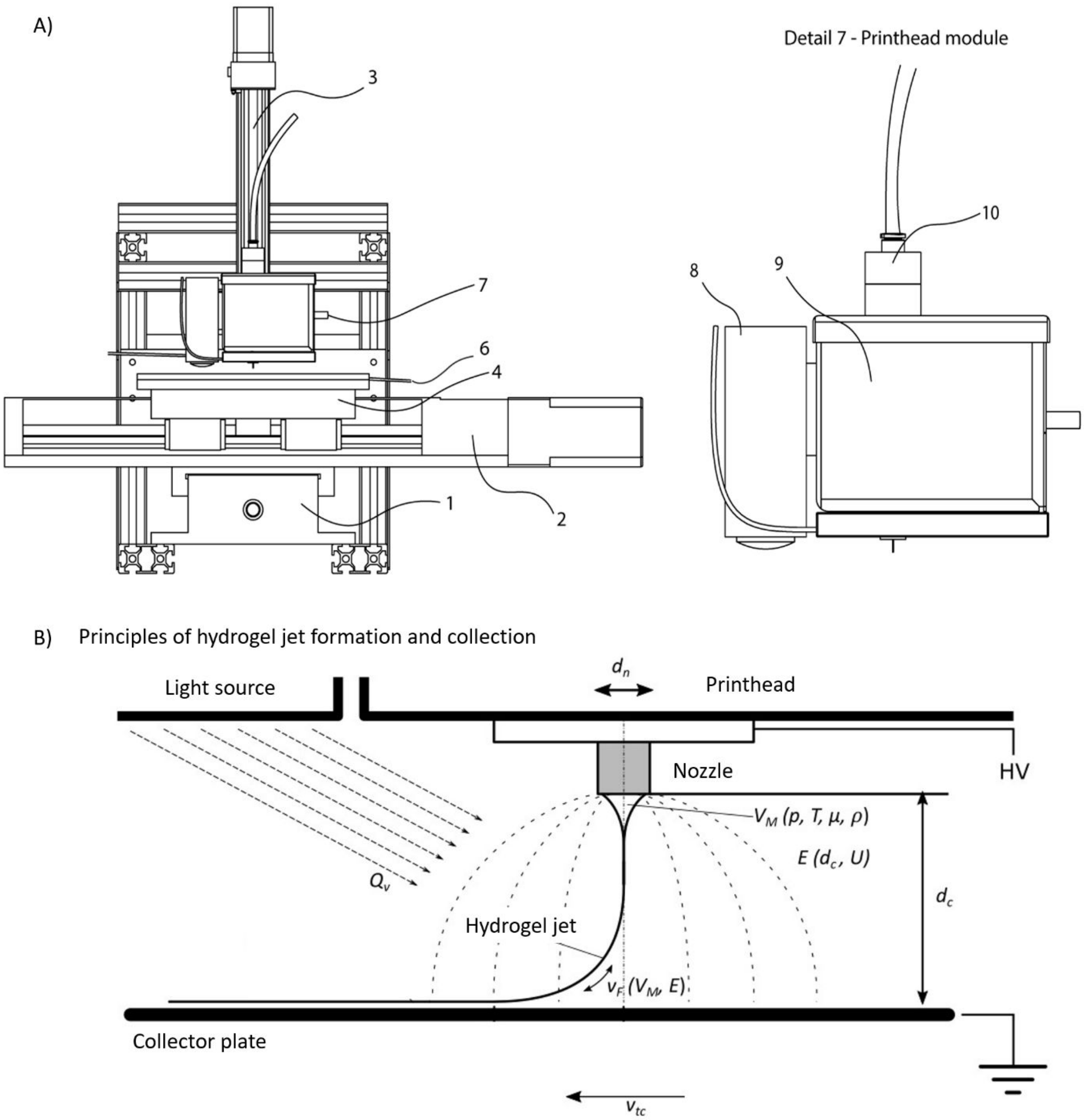

Figure S6: A) Schematic illustration of the custom-made CEW setup. The system comprises a XYZ computer controlled stage (1-4), a grounded aluminium collector plate (4-6), a printhead module for photo-crosslinkable inks (7) composed of a localized lighting source (8), a temperature controlled chamber (9) and a high precision air-pressure (10). B) Physics of CEW process. Governing mechanisms of hydrogel jet formation and collection during CEW are divided in two main steps, A) jet formation and B) jet collection and solidification. Jet formation starts by extruding a volume of a viscous hydrogel (V_M) that is then stretched by an applied electrical field (E) created between the dispensing nozzle (d_n) and collecting plate. V_M is dependent on extrusion pressure (p), hydrogel temperature (T), viscosity (μ) and electrical conductivity (ρ); while electrical field is a function of the collecting distance (d_c) and acceleration voltage (U). After jet formation, the hydrogel material solidifies by exposure to visible light (Qv) and straight hydrogel fibres are collected when the speed of the jet (v_f) equals the speed of the collector plate (v_{tc}).

Supplementary Tables and Table Captions

Table S1: Summary of electrohydrodynamic techniques using polymer and hydrogel solutions.

Electrohydrodynamic technique characteristics			**Material system**	**Cell characteristics**			**Mechanical properties**	**Ref**
System	Fiber size (µm)	Shape control	Composition	Cell encapsulation	Cell type	Viability (%)	Young modulus (MPa)	
SE	35 - 45	No	Polyvinyl alcohol	Yes	hMSCs	1.3- fold cell increase over 28d (proliferation only)	NE	1
SE	10 - 30	No	poly(dimethylsiloxane)	Yes	Astrocytes	67.7	NE	2
SE	0.3 – 0.5	No	Alginate w/ Polyethylene Oxide	Yes	HUVECs	90	0.004	3
SE	10	No	Alginate w/ Polyethylene Oxide	Yes	MSCs	60-80	0.07	4
SE	NE	No	Matrigel	Yes	Cardiomyocytes	80	NE	5
SE	NE	No	Matrigel	Yes	Mouse Neuroblastoma	80	NE	6
SE	0.8-5	No	Silkworm	NE	NE	NE	750	7
SE	1.2-2.4	No	Silkworm w/ Polyethylene Oxide	No	iPSC-MSCs	NE	24-1864	8
SE	70-100	Limited	Alginate w/ Polyethylene Oxide	Yes	Myoblasts	90	5	9
JW	120	Yes	poly(ethylene glycol) and poly(acrylic acid)	NE	NE	NE	NE	10
JW	6-50	Yes	poly(lactic-co-glycolic acid)	No	hMSCs	NE	NE	11
LEP	1-3	Limited	Polyethylene Oxide	Yes	Bacteria	NE	NE	12
LEP	2-4	Limited	Gelatin	NE	NE	NE	NE	13

LEP	1-10	Yes	Gelatin	No	Glioma cells	NE	20	14
NES	82.4	Yes	Alginate	Yes	HUVECs	95	NE	15
MEW	45	Yes	poly(2-ethyl-2-oxazine)	No	Fibroblasts	86	0.14 -0.20	16
MEW	73.9	Yes	Ureido-pyrimidinone-poly(ethylene glycol)	No	No	No	No	17
CEW	**3-6**	**Yes**	**Gelatin**	**Yes**	**MSCs**	**75**	**0.002**	**PW**
CEW	**40-45**	**Yes**	**Silk fibroin**	**Yes**	**MCSs**	**70**	**0.16**	**PW**

Abbreviations: SE, solution electrospinning; JW, 3D jet writing; LEP, ultralow voltage continuous electrospinning patterning; NES, near field electrospinning; MEW, melt electrowriting; CEW, cell electrowriting; hMSCs, Human mesenchymal stem cells; iPSCs-MSCs, Human-induced pluripotent stem cell - mesenchymal stem cells; HUVECs, Human umbilical vein endothelial cells; NE, not evaluated; PW, present work

References

(1) Chen, H.; Liu, Y.; Hu, Q. A Novel Bioactive Membrane by Cell Electrospinning. *Exp. Cell Res.* 338, 261-266. 2015. https://doi.org/10.1016/j.yexcr.2015.08.007.

(2) Townsend-Nicholson, A.; Jayasinghe, S. N. Cell Electrospinning: A Unique Biotechnique for Encapsulating Living Organisms for Generating Active Biological Microthreads/Scaffolds. *Biomacromolecules* 7, 3364-9. 2006. https://doi: 10.1021/bm060649h

(3) Yeo, M.; Kim, G. H. Micro/Nano-Hierarchical Scaffold Fabricated Using a Cell Electrospinning/3D Printing Process for Co-Culturing Myoblasts and HUVECs to Induce Myoblast Alignment and Differentiation. *Acta Biomater.* 107, 102-114. 2020. https://doi.org/10.1016/j.actbio.2020.02.042.

(4) Yeo, M. G.; Kim, G. H. Fabrication of Cell-Laden Electrospun Hybrid Scaffolds of Alginate-Based Bioink and PCL Microstructures for Tissue Regeneration. *Chem. Eng. J.* 275, 27-35. 2015. https://doi.org/10.1016/j.cej.2015.04.038.

(5) Ehler, E.; Jayasinghe, S. N. Cell Electrospinning Cardiac Patches for Tissue Engineering the Heart. *Analyst*. 139, 4449-4452. 2014. https://doi.org/10.1039/c4an00766b.

(6) Sampson, S. L.; Saraiva, L.; Gustafsson, K.; Jayasinghe, S. N.; Robertson, B. D. Cell Electrospinning: An in Vitro and in Vivo Study. *Small*. 10, 1, 1300804. 2014. https://doi.org/10.1002/smll.201300804.

(7) Wang, M.; Jin, H. J.; Kaplan, D. L.; Rutledge, G. C. Mechanical Properties of Electrospun Silk Fibers. *Macromolecules*. 37, 6856-6864. 2004. https://doi.org/10.1021/ma048988v.

(8) Yi, B.; Zhang, H.; Yu, Z.; Yuan, H.; Wang, X.; Zhang, Y. Fabrication of High Performance Silk Fibroin Fibers: Via Stable Jet Electrospinning for Potential Use in Anisotropic Tissue Regeneration. *J. Mater. Chem. B*. 6, 3934-3945. 2018. https://doi.org/10.1039/c8tb00535d.

(9) Yeo, M.; Kim, G. H. Anisotropically Aligned Cell-Laden Nanofibrous Bundle Fabricated via Cell Electrospinning to Regenerate Skeletal Muscle Tissue. *Small* 14, 1803491. 2018. https://doi.org/10.1002/smll.201803491.

(10) Steier, A.; Schmieg, B.; Irtel von Brenndorff, Y.; Meier, M.; Nirschl, H.; Franzreb, M.; Lahann, J. Enzyme Scaffolds with Hierarchically Defined Properties via 3D Jet Writing. *Macromol. Biosci.* 20, 2000154. 2020. https://doi.org/10.1002/mabi.202000154.

(11) Jordahl, J. H.; Solorio, L.; Sun, H.; Ramcharan, S.; Teeple, C. B.; Haley, H. R.; Lee, K. J.; Eyster, T. W.; Luker, G. D.; Krebsbach, P. H.; Lahann, J. 3D Jet Writing: Functional Microtissues Based on Tessellated Scaffold Architectures. *Adv. Mater.* 30, 14, 1707196. 2018. https://doi.org/10.1002/adma.201707196.

(12) Li, X.; Li, Z.; Wang, L.; Ma, G.; Meng, F.; Pritchard, R. H.; Gill, E. L.; Liu, Y.; Huang, Y. Y. S. Low-Voltage Continuous Electrospinning Patterning. *ACS Appl. Mater. Interfaces*. 8, 32120-32131. 2016. https://doi.org/10.1021/acsami.6b07797.

(13) Gill, E. L.; Wang, W.; Liu, R.; Huang, Y. Y. S. Additive Batch Electrospinning Patterning of Tethered Gelatin Hydrogel Fibres with Swelling-Induced Fibre Curling. *Addit. Manuf.* 36, 101456. 2020. https://doi.org/10.1016/j.addma.2020.101456.

(14) Gill, E. L.; Willis, S.; Gerigk, M.; Cohen, P.; Zhang, D.; Li, X.; Huang, Y. Y. S. Fabrication of Designable and Suspended Microfibers via Low-Voltage 3D Micropatterning. *ACS Appl. Mater. Interfaces* 11, 19679-19690. 2019. https://doi.org/10.1021/acsami.9b01258.

(15) He, J.; Zhao, X.; Chang, J.; Li, D. Microscale Electro-Hydrodynamic Cell Printing with High Viability. *Small*. 13, 47, 1702626. 2017. https://doi.org/10.1002/smll.201702626.

(16) Nahm, D.; Weigl, F.; Schaefer, N.; Sancho, A.; Frank, A.; Groll, J.; Villmann, C.; Schmidt, H.-W.; Dalton, P. D.; Luxenhofer, R. A Versatile Biomaterial Ink Platform for the Melt Electrowriting of Chemically-Crosslinked Hydrogels. *Mater. Horizons. 3.* 2020. https://doi.org/10.1039/C9MH01654F.

(17) Wu, D. J.; Vonk, N. H.; Lamers, B. A. G.; Castilho, M.; Malda, J.; Hoefnagels, J. P. M.; Dankers, P. Y. W. Anisotropic Hygro-Expansion in Hydrogel Fibers Owing to Uniting 3D Electrowriting and Supramolecular Polymer Assembly. *Eur. Polym. J.* 141, 110099. 2020. https://doi.org/10.1016/j.eurpolymj.2020.110099.